

- Conference on the Physics of Semiconductors, Exeter*, 1962, edited by A. C. Strickland (The Institute of Physics and the Physical Society, London, 1962), p. 659.
- <sup>8</sup>B. Yates, *J. Electron. Control* **6**, 26 (1959).
- <sup>9</sup>Kimio Hashimoto, *J. Phys. Soc. Japan* **16**, 1970 (1961).
- <sup>10</sup>G. F. Koster, in *Solid State Physics*, edited by F. Seitz and D. Turnbull (Academic, New York, 1957), Vol. 5, p. 174.
- <sup>11</sup>J. R. Drabble and R. Wolfe, *Proc. Phys. Soc. (London)* **69**, 1101 (1956).
- <sup>12</sup>I. G. Austin, *Proc. Phys. Soc. (London)* **76**, 169 (1960).
- <sup>13</sup>F. Borghese and E. Donato, *Nuova Cimento* **53B**, 283 (1968).
- <sup>14</sup>D. L. Greenaway and G. Harbeke, *J. Phys. Chem. Solids* **26**, 1585 (1965).
- <sup>15</sup>Shin-ichi Katsuki, *J. Phys. Soc. Japan* **26**, 58 (1969).
- <sup>16</sup>Robert W. Keyes, *J. Electron. 2*, 279 (1956).
- <sup>17</sup>J. R. Drabble, *Proc. Phys. Soc. (London)* **72**, 380 (1958).
- <sup>18</sup>Arthur C. Smith, James F. Janak, and Richard B. Adler, *Electronic Conduction in Solids* (McGraw-Hill, New York, 1967).
- <sup>19</sup>D. J. Howarth, E. H. Sondheimer, *Proc. Roy. Soc. (London)* **A219**, 53 (1953).
- <sup>20</sup>Conyers Herring, *Bell System Tech. J.* **34**, 237 (1955).
- <sup>21</sup>Albert C. Beer, *Solid State Physics, Suppl. 4, Galvanomagnetic Effects in Semiconductors*, edited by F. Seitz and D. Turnbull (Academic, New York, 1963), Sec. 25.
- <sup>22</sup>Conyers Herring and Erich Vogt, *Phys. Rev.* **101**, 944 (1956).
- <sup>23</sup>R. S. Allgaier, *Phys. Rev.* **165**, 775 (1968).
- <sup>24</sup>I. Ya. Korenblit, *Fiz. Tverd. Tela* **2**, 3083 (1960) [*Soviet Phys. Solid State* **2**, 2738 (1961)].
- <sup>25</sup>B. A. Efimova, I. Ya. Korenblit, V. I. Novikov, and A. G. Ostroumov, *Fiz. Tverd. Tela* **3**, 2746 (1961) [*Soviet Phys. Solid State* **3**, 2004 (1962)].
- <sup>26</sup>H. J. Mackey and J. R. Sybert, *Phys. Rev.* **180**, 678 (1969).
- <sup>27</sup>B. D. Cullity, *Elements of X-Ray Diffraction*, (Addison Wesley, Reading, Mass., 1956).
- <sup>28</sup>A. Sagar and J. W. Faust, Jr., *J. Appl. Phys.* **38**, 482 (1967).
- <sup>29</sup>John G. Herriot, *Methods of Mathematical Analysis and Computation* (Wiley, New York, 1963), p. 73.
- <sup>30</sup>A. M. Ostrowski, *Solution of Equations and Systems of Equations* (Academic, New York, 1966), p. 183.
- <sup>31</sup>P. Drath and G. Landwehr, *Phys. Letters* **24A**, 504 (1967).
- <sup>32</sup>P. Drath, *Z. Naturforsch.* **23A**, 1146 (1968).
- <sup>33</sup>Charles Kittel, *Introduction to Solid State Physics* (Wiley, New York, 1956), 2nd ed.
- <sup>34</sup>V. L. Bonch-Bruyevich, *The Electronic Theory of Heavily Doped Semiconductors* (Elsevier, New York, 1966), p. 88.
- <sup>35</sup>B. A. Efimova, V. I. Novikov, and A. G. Ostroumov, *Fiz. Tverd. Tela* **4**, 302 (1962) [*Soviet Phys. Solid State* **4**, 218 (1963)].
- <sup>36</sup>Gerald R. Miller, Masters thesis, Cornell University, 1963 (unpublished); G. R. Miller, Che-Yu Li, and C. W. Spencer, *J. Appl. Phys.* **34**, 1398 (1963).
- <sup>37</sup>R. F. Broom, *Proc. Phys. Soc. (London)* **71**, 500 (1958).
- <sup>38</sup>J. R. Drabble and R. Wolfe, *J. Electron. Control* **3**, 259 (1957).

## Anharmonicity and the Temperature Dependence of the Forbidden (222) Reflection in Silicon†

J. B. Roberto\* and B. W. Batterman

*Department of Materials Science and Engineering, Cornell University, Ithaca, New York 14850*

(Received 29 April 1970)

The temperature dependence of the integrated intensity of the forbidden (222) reflection in silicon has been measured from 4 to 900 °K. The results indicate that the (222) intensity at room temperature is due almost entirely to charge asymmetries introduced by the covalent bonds. However, the temperature dependence may be due to a combination of bond vibrations and anharmonicity in the atom motions. From estimates of the anharmonic contribution, and the observed temperature dependence, there is evidence that the thermal motion of the covalent bond may be different from that of the core electrons. The absolute intensity of the (222) was also measured and is consistent with  $F(222) = 1.46 \pm 0.04$ .

### I. INTRODUCTION

In Bragg diffraction, a reflection with zero structure factor for the unit cell is termed forbidden. In the diamond structure, reflections with  $h, k, l$  mixed or  $h, k, l$  an odd multiple of 2 should be forbidden from a lattice point consideration. Nevertheless, in 1921 Bragg<sup>1</sup> found a weak x-ray re-

flection at the forbidden (222) position in diamond.

Silicon crystallizes in the diamond structure, and a similar anomalous reflection appears at the (222). Since spherical atoms at the lattice sites yield a zero structure factor, this forbidden intensity must be due to some perturbation on the spherical atoms. Further, since the x rays interact only with the electron charge distribution of an atom,

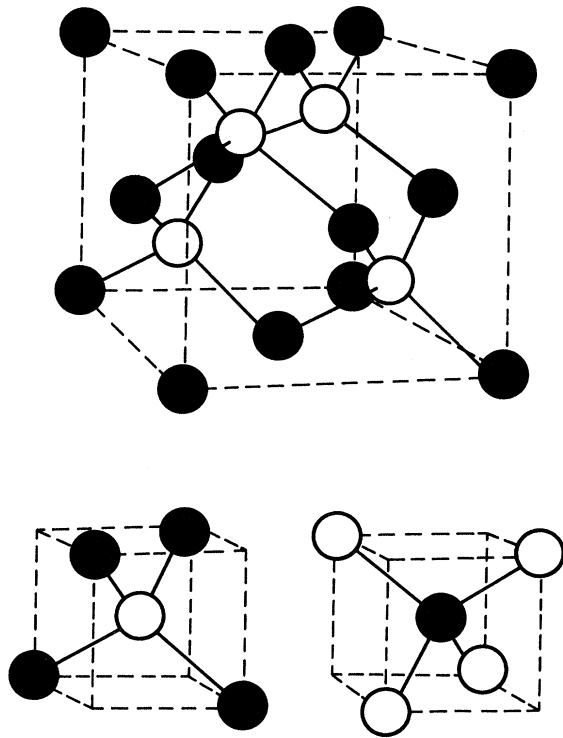


FIG. 1. Diamond structure: The shaded atoms represent one fcc lattice. The inversion of bond orientations in the two fcc sublattices is illustrated in the two smaller cubes.

this perturbation must show up as an asymmetry in the charge cloud. Silicon and diamond are covalent crystals, and some portion of this asymmetry might be expected in bonding effects.

Another possible asymmetry can arise even from spherically symmetrical atomic electrons. In the diamond structure (Fig. 1), each atom has a tetrahedral environment. Because of this, each atom sees a bond (and nearest neighbor) in one direction and a "hole" in the opposite direction along any (111) axis. It is reasonable to assume, particularly at higher temperatures, that an atom would spend more of its time toward the hole than toward the bond. This anharmonicity in atom motions would create a time-averaged asymmetry and produce a core contribution to the (222) reflection. In three dimensions, this introduces a tetrahedral symmetry to the spherical atoms. One can approximate this anharmonic motion by replacing the lattice sites with four atoms, each with  $\frac{1}{4}$  the scattering power of the original atom and each displaced from the lattice sites in tetrahedral fashion by an anharmonic displacement  $\delta$  along the appropriate  $\langle 111 \rangle$  direction.<sup>2</sup> A calculation for this new "quarter-ion" lattice yields an anharmonic structure factor for the forbidden reflections of the type  $h+k+l=4n\pm 2$ ,

$$F_{\text{anh}} = (2\pi\delta)^3 (hkl) 8fe^{-M}, \quad (1)$$

where  $(hkl)$  is the product of the Miller indices,  $f$  the atomic scattering factor, and  $e^{-M}$  the Debye-Waller factor. The (222) reflection in neutron diffraction should be sensitive only to the core motion of the atom. This follows because the scattering will only be from an effective point nucleus and any asphericity in the electron cloud would not be detected. Recent neutron measurements<sup>3</sup> have failed to detect any (222) reflection due to anharmonic motion.

Tetrahedral symmetry in the charge cloud may be introduced into the atom by considering the covalent bond to consist of small lobes of charge extending in the bond direction. Locating point charges of scattering factor  $f_e$  a distance  $\delta$  in the bond directions reminds us of the quarter-ion model, and yields a structure factor similar to Eq. (1) but with opposite sign to that due to anharmonic displacements.

The core and bonding contributions are quite similar, each arising from a tetrahedral deformation of spherical atoms by anharmonic motion or bonds. The forbidden reflections occur not because of this deformation alone, but because of the particular orientation of the tetrahedra with respect to each other. Referring again to Fig. 1, it can be seen that the tetrahedral deformations invert with each successive atomic plane in a (111) direction. It is this inversion which creates the necessary charge asymmetry for the forbidden reflections to appear.

When considered together, the core and bonding effects tend to work against each other. At a particular atom, the orientations of the anharmonic and bonding tetrahedra are opposite. Hence, the necessary inversion from plane to plane of one contribution is reduced by the opposite inversion of the other. Another way of putting this is that the two effects acting simultaneously tend to make the time-averaged charge distribution more spherical. If both the effects of anharmonicity and bonding are present in the (222), it might be expected that the bonds would dominate at lower temperatures and the anharmonic or core contribution would become more prevalent as increased temperature allows more thermal motion.

The existence of the (222) has been known for almost 50 years, and experimental values for the structure factor of the forbidden reflection in silicon have varied from less than 1.0 to almost 2. Moreover, no conclusive data on the relative importance of bonding and core contributions to the (222) has been forwarded. In fact, it is only recently that anharmonic effects have even been considered. From the negative neutron diffraction experiments,

it is to be expected that the forbidden reflection is due mainly to the bonding electrons, and that the absolute intensity of the (222) can be used as a check on the accuracy of electronic band-structure calculations which predict outer-electron wave functions.<sup>4-6</sup> The (222) offers a special advantage here over allowed reflections since the bonding contribution is not masked by the very nearly spherical core electron distribution.

In this experiment, it is undertaken to sort out the bonding and core contributions to the (222). A temperature approach was chosen for this objective. While one can only speculate on the temperature dependence of a covalent bond, it is clear that the anharmonicity necessary for the core contribution would be strongly temperature dependent. As an experimental by-product of the temperature work, the absolute intensity of the forbidden reflection was also measured.

## II. EXPERIMENTAL

The (222) is two orders of magnitude weaker than allowed reflections in silicon, and care must be exercised to insure an accurate measurement. A large source of possible experimental error is multiple reflections. In 1937, Renninger<sup>7</sup> noticed that the intensity of the forbidden reflection changed as the crystal was rotated in azimuth about the normal to the diffracting planes. This "umweganregung" effect occurs when conditions for simultaneous or multiple reflection are satisfied. The azimuthal position of multiple-reflection contributions to the (222) intensity can be readily ascertained by comparing an experimental azimuthal scan with a computer-predicted umweganregung pattern (Cole *et al.*).<sup>8</sup> Figure 2(a) shows an azimuthal scan with the diffraction vector close to the (222) reciprocal-lattice point. The pattern repeats every 30°. The indices shown for peaks 1-5 represent the reflec-

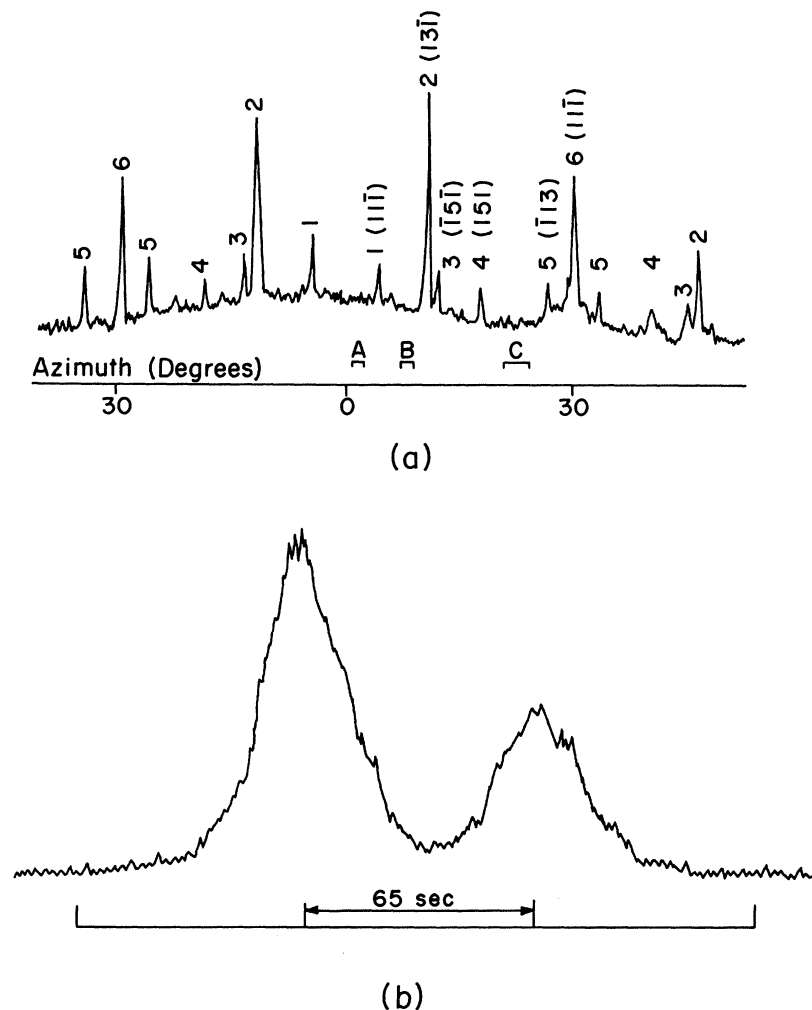


FIG. 2. (a) Experimental umweganregung pattern. The diffraction vector corresponds to the (222) reflection and the crystal is rotated about this vector. The variation in background or "true" (222) intensity is due to slight wobble in the azimuthal rotation. Regions of umweganregung-free (222) used in the intensity measurements are denoted by A, B, and C. (b) (222) rocking curve showing  $\alpha_1$  and  $\alpha_2$  peaks taken at azimuthal position A in Fig. 2(a).  $\alpha_1$  peak intensity is about 200 cps.

tion other than the (222) which lies on the Ewald sphere of the primary beam. A, B, and C are the regions free of multiple reflections used in the present measurements. The background is the "true" (222) intensity, the variation of which is due to wobble in the azimuthal rotation axis.

Another consideration is the possible introduction of strains and imperfections in the crystals during heating and cooling. Perfect single crystals of silicon (Lopex) with dislocation densities  $< 100 \text{ cm}^{-2}$  were used in the measurement primarily because they concentrate more reflecting power in a narrower angular range than mosaic crystals and hence lead to greater peak intensities.

Thermal strain could easily alter the integrated intensities by making the diffraction process more kinematic. Intensity ratios of a factor of 5 are not uncommon between ideally perfect and mosaic crystals. This effect however is important only for strong reflections. The difference in integrated intensity between ideally perfect and imperfect is less than 2% for the weak (222), and thermal strains should not be important.

The integrated intensities were measured on a double crystal spectrometer of Bond design.<sup>9</sup> A perfect (220) silicon first crystal was chosen to provide a strong primary beam and sufficient dispersion for reasonably attainable umweganregung patterns. The Cu  $K\alpha$  radiation yielded the best combination of intensity and umweganregung-free regions. Slits were fairly open, allowing a beam approximately 1 mm in width (allowing the entire x-ray focal spot to be used) and 3 mm in height to fall upon the second crystal. Peak intensities of the order of 200 counts/sec with an  $\alpha_1$ - $\alpha_2$  separation of 65 sec of arc were observed for the true (222). A characteristic (222) rocking curve is shown in Fig. 2(b).

A scintillation counter was used for most of the measurements although similar results were also obtained with proportional counters. A single-channel analyzer was set for the  $K\alpha$  peak and excluded short-wavelength harmonics.

The absolute intensity of the (222) was measured relative to the (111) and (333). Well-established structure factors are available for the (111) and (333) so the problem of measuring the direct beam was avoided. Direct-beam measurement would be very difficult because of the wide-open slit system used. Calibrated foils which attenuated the reflected beam by factors of approximately 32 and 8 were used to bring the intensities of the allowed reflections into countable regions.

The angular range used for determining integrated intensities was of three  $\alpha_1$ - $\alpha_2$  spacings: from one  $\alpha_1$ - $\alpha_2$  separation before the  $\alpha_1$  peak to one beyond the  $\alpha_2$  peak. Background levels were taken at both

extremities of the rocking curve and subtracted from the total intensity. By comparison with rocking curves covering a much wider angular range, it was determined that approximately 3% of the integrated intensity was left uncounted in the tails of the peaks because of the relatively short ( $3\alpha_1$ - $\alpha_2$  spacings) scan and the correction was taken into account in the final result. Rocking curves for the (111) and (333) covered similar angular ranges based on their  $\alpha_1$ - $\alpha_2$  separation, insuring an accurate relative measurement. Integrated intensities were taken at three different umweganregung-free azimuths [A, B, and C in Fig. 2(a)] in  $180^\circ$  pairs to compensate for any crystal miscut. In all, more than 400 000 counts of (222) were measured in about 30 scans. These data were compared with approximately 20 rocking curves at the (111) and 8 at the (333).

All temperature runs were made relative to the room-temperature (222), a number of rocking curves at a given temperature were followed by the same number at room temperature. Three different crystals were used and at least three different umweganregung-free azimuths measured.

Low temperature runs were made at liquid-helium and liquid-nitrogen temperatures, with the crystal mounted on a copper cold finger in an evacuated cryostat similar to one previously described in the literature.<sup>10</sup> The high-temperature measurement was made up to  $600^\circ\text{C}$  in a helium-purged baffle furnace.<sup>11</sup> Three Chromel-Alumel thermocouples were placed near or touching the back of the crystal at various locations and consistently read within  $10^\circ$  of each other.

Since the intensities always returned to the same room-temperature value after a high-temperature run, it was concluded that the effects of any surface contamination were negligible. Approximately 400 000 counts were taken at each temperature (both low and high) in about 40 rocking curves.

### III. RESULTS

The data for absolute intensity measurements consisted of ratios of the experimental integrated intensities of the (111), (222), and (333) reflections. Using previously determined values<sup>12</sup> for  $F(111) = 62.2$  and  $F(333) = 33.2$ , and the above measured ratios, the (222) structure factor was determined. A structure factor was computed for each independently measured ratio, three (222) and (111) measurements and three (222) and (333) measurements. Each individual measurement consisted of the average of several rocking curves at three or more different azimuths. These computed structure factors then were averaged and to within one standard deviation yielded an  $F(222)$  for the unit cell of  $1.46 \pm 0.04$ . The dynamical Darwin-Prins equa-

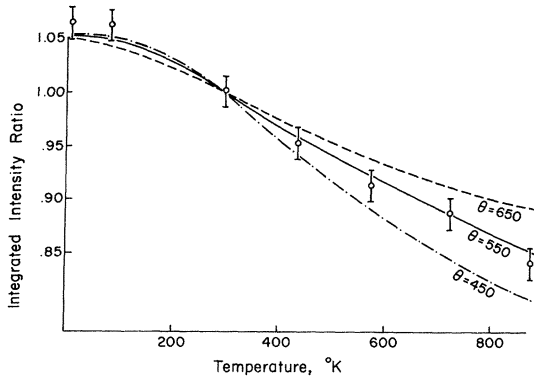


FIG. 3. Ratio of experimental integrated intensity at temperature  $T$  to room temperature. The curves are the ratios of the Debye-Waller factors  $e^{-2M}$  for different Debye temperatures.

tion<sup>13</sup> was used for this calculation. The linear absorption coefficient for Cu  $K\alpha$  in silicon was taken as  $144 \text{ cm}^{-1}$ .<sup>14</sup> This result compares well with experimental room-temperature values for the (222) of DeMarco and Weiss ( $1.44 \pm 0.08$ ),<sup>15</sup> of Colella and Merlini (1.54),<sup>16</sup> and of Renninger (1.55)<sup>17</sup> and is in fair agreement with that of Wolfel *et al.* (1.78).<sup>18</sup>

The temperature results are represented by the brackets in Fig. 3. Each measurement consisted of approximately ten rocking curves at both room and the given temperature for a particular azimuth. Then the results for different azimuths and crystals at a given temperature were combined. The quoted precision represents fluctuations of approximately one standard deviation.

#### IV. DISCUSSION

The temperature results in Fig. 3 indicate that the intensity of the forbidden reflection decreases as temperature is increased. This suggests that the (222) is due primarily to bonding effects, since the intensity due to anharmonicity alone would be expected to increase with temperature.

Neglecting anharmonic motion, an x-ray beam at the (222) does not diffract from the core electron distribution. Instead, it sees only the bonds, an array of charge lobes slightly displaced in tetrahedral fashion from the lattice points. The effect of temperature would be to blur this array by subjecting individual lobes to random displacements. These displacements tend to impair phase relationships, and reduce the intensity of a reflection by a factor  $e^{-2M}$ ,<sup>19</sup> where  $M$  is the Debye-Waller factor. For a Debye model,

$$M = 8\pi^2 \langle u_s^2 \rangle [(\sin\theta)/\lambda]^2, \quad (2)$$

$$\langle u_s^2 \rangle = \frac{3}{4} (\hbar^2 T / mk\Theta^2 \pi^2) [\Phi(x) + \frac{1}{4}x], \quad (3)$$

where  $\langle u_s^2 \rangle$  is the mean squared amplitude of vibration,  $\hbar$  is Planck's constant,  $m$  is the atomic mass,  $k$  the Boltzmann constant,  $\Theta$  the characteristic or Debye temperature,  $x = \Theta/T$ , and  $[\Phi(x) + \frac{1}{4}x]$  the Debye function which takes into account the zero-point motion.

In Fig. 3, the measured temperature dependence of the forbidden reflection is compared with theoretical  $e^{-2M}$  dependences for several Debye temperatures. The data agree well with theory over the entire temperature range for the experimental x-ray Debye temperature of silicon,<sup>20</sup>  $\Theta = 543^\circ \text{K}$ . At first glance then, it would appear that the entire temperature behavior of the (222) can be described in a very straightforward way. Namely, the (222) is due to bond electrons which vibrate with the same harmonic vibrational amplitude as the core electrons and nucleus.

We will consider the effect of anharmonicity according to the formalism developed by Dawson and Willis.<sup>21</sup> The complete temperature dependence of the anharmonic contribution is calculated by assuming that each atom vibrates in an anharmonic potential well of the form

$$V = V_0 + \alpha(x^2 + y^2 + z^2) + \beta xyz, \quad (4)$$

with  $\alpha$  and  $\beta$  constants.

This well has the required symmetry (spherical with tetrahedral lobes), and to third order represents the best approximation to the actual potential. An ensemble average of the temperature factor<sup>22</sup> using the above potential yields a high temperature or classical anharmonic structure factor for the  $h+k+l = 4n+2$  reflections

$$F_{\text{anh}} = (kT)^2 (2\pi/a)^3 (\beta/\alpha^3) (hkl) 8fe^{-M}, \quad (5)$$

where  $a$  is the dimension of the unit cell,  $f$  is the atomic scattering factor,  $kT$  is the Boltzmann factor times absolute temperature, and the additional symbols have been defined above. Comparing Eqs. (5) and (1),  $\delta$  for the quarter-ion model can be expressed in terms of the potential-well parameters as  $\delta^3 = (kT)^2 \beta / (a\alpha)^3$ . The coefficient  $\alpha$  can be derived from the Debye-Waller factor<sup>21</sup> which yields the high-temperature result

$$\alpha = kT / \langle u_s^2 \rangle = 7.85 \times 10^{-12} \text{ erg}/\text{\AA}^2, \quad (6)$$

using a Debye  $\Theta = 543^\circ \text{K}$  and Eq. (3).

Thus, to evaluate  $F_{\text{anh}}$  we need an estimate of  $\beta$ , the cubic term in the potential. An approximate value is obtained from the linear expansion coefficient by a model in which a pair of silicon neighbors is treated as an independent diatomic model and the anisotropic term in the potential changes the equilibrium separation with temperature. This simplified approach yields<sup>21</sup>

$$|\beta|/\alpha = 3\alpha\chi\alpha/4k = 1.03 \text{ \AA}^{-1}, \quad (7)$$

where the only undefined symbol  $\chi$  is the linear thermal-expansion coefficient. The total structure factor incorporating both the bonding contribution and the anharmonic effects now becomes

$$F(222) = F_b - F_{\text{anh}} = F_b - (kT)^2 [\Phi(x) + \frac{1}{4}x]^2 \times (2\pi/a)^3 (\beta/\alpha^3) (hkl) 8fe^{-M}. \quad (8)$$

The function  $[\Phi(x) + \frac{1}{4}x]^2$  is included in the second (anharmonic term) to approximate the low-temperature behavior of  $\alpha$ . This follows from Eqs. (3) and (6) by including the temperature-independent zero-point vibrational amplitude. In this approximation,  $\alpha$  is considered a constant in Eq. (8) with the value given by Eq. (6). Because of the origin of their respective contributions,  $F_b$  and  $F_{\text{anh}}$  will always be of opposite sign. Using Eq. (8) for  $F_{\text{anh}}$ ,  $F_b$  is determined so that  $F(222)$  is the experimental room-temperature value.

We now assume that  $F_b$  is independent of temperature, i.e., that the bonding electrons have no thermal vibrations and calculate the temperature dependence of  $[F(222)]^2$ , which is proportional to the integrated intensity. In Fig. 4 we show the results of this calculation for several values of  $\beta/\alpha$  in the vicinity of the value of  $1.03 \text{ \AA}^{-1}$  estimated in Eq. (7). The curve for  $\beta/\alpha = 1.0$  is a reasonable fit to the data from room temperature to about  $800^\circ\text{K}$ . This rather unexpected result says that experimental data are reasonably consistent with a model in which the valence electrons do not vibrate thermally but that the temperature dependence of the (222) is due almost entirely to anharmonic vibrations of the core electrons. This of course is based upon a very rough estimation of  $\beta$ , the anharmonic cubic

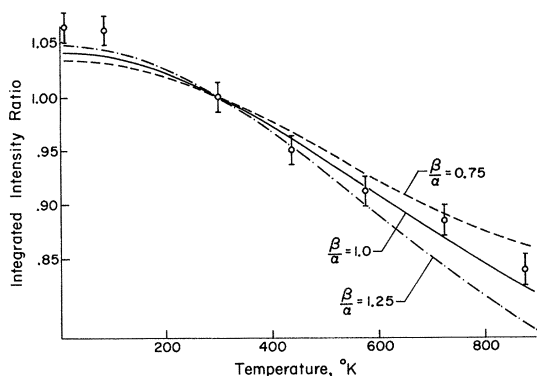


FIG. 4. Temperature dependence of the (222) for several values of  $\beta/\alpha (\text{\AA}^{-1})$ . In this case, the bonds are assumed not to vibrate and the temperature effect is solely due to anharmonicity. Brackets represent experimental data.

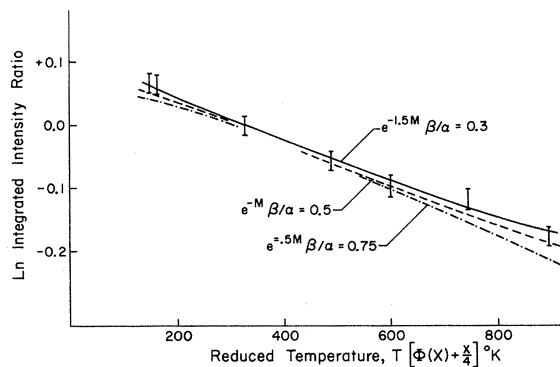


FIG. 5. Three possible combinations of anharmonic and bonding effects consistent with the observed temperature dependence.

term in the potential. For  $\beta/\alpha = 1.0$ , the anharmonic contribution at room temperature is only about 2% of  $F(222)$ , so it is quite clear that the (222) results primarily from the nonspherical distribution of bonding electrons about the atom. However, the  $T^2$  dependence of the anharmonic term alone is strong enough to decrease the structure factor with temperature to be consistent with experimental results.

This argument is crucially dependent on the value of  $\beta$ . While Dawson and Willis's<sup>21</sup> qualitative arguments give  $\beta/\alpha = 1.03$ , the experimental neutron diffraction work by Nunes<sup>3</sup> suggests that  $\beta/\alpha$  may be less than half this value. The experiment failed to find a neutron nuclear (222) reflection, which from estimates of experimental accuracy would require  $\beta/\alpha \leq 0.6 \text{ \AA}^{-1}$ .

It is clear from the above discussion that two quite different explanations are consistent with the observed temperature dependence of the forbidden (222) reflection. One which has the bonding electrons vibrating harmonically with the core of the atom and the other which postulates stationary valence electrons and an anharmonically vibrating atom.

It is also evident that many combinations of the two models can be made consistent with experiment. In Fig. 5, we give as an illustration three combinations. The log of the intensity versus  $T[\Phi(x) + \frac{1}{4}x]$  makes the plots nearly linear. The solid line which gives a good fit over the entire range has a  $\beta/\alpha = 0.3$  and has roughly a 25% reduction in the mean square amplitude of the bonding electrons over that of the core. The fit using  $\beta/\alpha = 0.5$  and a 50% reduction is a good fit above room temperature. The curves are not to be taken too seriously but are included to show the range of models that could be consistent with experiment.

## V. CONCLUSIONS

The experimental results indicate strongly that the forbidden (222) reflection in silicon at room temperature is due almost entirely to the asphericity of the bonding electrons. The anharmonic contribution at this temperature is probably less than 5% of the total integrated intensity. The results are inconclusive as to the origin of the temperature dependence of the (222). Several combinations of bonding and anharmonic effects can be made consistent with the observed temperature dependence. Two extreme models would explain the data. In one, the bonding electrons vibrate the same as the core electrons. In the other, the tetrahedral bonding charge does not vibrate at all and the entire temperature dependence is due to anharmonic atom

vibrations of the silicon atoms.

It is therefore unwarranted at this time to say anything definitive about the reasons for the temperature dependence of the (222). The key to the problem is the value of the anharmonicity parameter  $\beta$ . The method of estimating  $\beta$  for silicon is similar to that used for ionic crystals<sup>23</sup> which gave results for the latter in reasonable agreement with experiment. These  $\beta$  values for silicon provide for a significant anharmonic contribution to the (222) temperature dependence and would lead to the conclusion that the vibrational amplitude of the bonding electrons in silicon is less than that of core electrons. An experimental measurement of the anharmonic  $\beta$  parameter is essential to unraveling the bond electron motion in silicon.

<sup>†</sup>Work supported by the Advanced Research Projects Administration through the Materials Science Center at Cornell University, Ithaca, N. Y.

\*This work is the result of thesis research for the requirement of Master of Science in Applied Physics. Present address: U. S. Marine Corps.

<sup>1</sup>W. H. Bragg, *Proc. Phys. Soc. (London)* **33**, 304 (1921).

<sup>2</sup>This is similar to the approximation used by B. T. M. Willis [*Acta Cryst.* **18**, 75 (1965)] to describe the anharmonic vibration of the F atom in CaF<sub>2</sub>.

<sup>3</sup>A. C. Nunes, *Acta Cryst.* (to be published).

<sup>4</sup>L. Kleinman and J. C. Phillips, *Phys. Rev.* **125**, 819 (1962).

<sup>5</sup>R. Brill *et al.*, *Ann. Physik* **34**, 393 (1939).

<sup>6</sup>E. Lafon, Quarterly Progress Report of the Solid-State and Molecular Theory Group, M. I. T., 1968, Vol. 69, p. 66 (unpublished).

<sup>7</sup>M. Renninger, *Z. Physik* **106**, 141 (1937).

<sup>8</sup>H. Cole, F. Chambers, and H. Dunn, *Acta Cryst.* **15**, 138 (1962).

<sup>9</sup>W. L. Bond, *Rev. Sci. Instr.* **39**, 1434 (1968).

<sup>10</sup>B. W. Batterman and C. S. Barrett, *Phys. Rev.*

**145**, 296, 1966.

<sup>11</sup>B. W. Batterman, *Phys. Rev.* **126**, 1461 (1962).

<sup>12</sup>H. Hattori *et al.*, *J. Phys. Soc. Japan* **20**, 988 (1965).

<sup>13</sup>P. B. Hirsch and G. N. Ramachandran, *Acta Cryst.* **3**, 187 (1950).

<sup>14</sup>L. D. Jennings (private communication).

<sup>15</sup>J. J. DeMarco and R. J. Weiss, *Phys. Rev.* **137**, A1869 (1965).

<sup>16</sup>R. Colella and A. Merlini, *Phys. Status Solidi* **18**, 157 (1966).

<sup>17</sup>M. Renninger, *Z. Krist.* **113**, 99 (1960).

<sup>18</sup>E. Wolfel *et al.*, *Z. Physik Chem. (Frankfurt)* **21**, 133 (1959).

<sup>19</sup>R. W. James, *The Optical Principles of the Diffraction of X-Rays* (Cornell U. P., Ithaca, N. Y., 1965), pp. 193-230.

<sup>20</sup>B. W. Batterman and D. R. Chipman, *Phys. Rev.* **127**, 690 (1962).

<sup>21</sup>B. Dawson and B. T. M. Willis, *Proc. Roy. Soc. (London)* **298**, 307 (1967).

<sup>22</sup>B. T. M. Willis, *Acta Cryst.* **A25**, 277 (1969).

<sup>23</sup>B. Dawson, A. C. Hurley, and V. W. Maslen, *Proc. Roy. Soc. (London)* **A298**, 289 (1967).